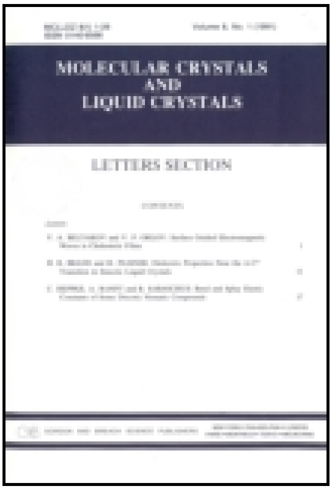

Molecular Crystals and Liquid Crystals
Publication details, including instructions for authors and subscription information:
http://www.tandfonline.com/loi/gmcl20

Thermomechanical Effects in Hybrid and Cylindrical-Hybrid Oriented Nematic Liquid Crystals

Mariam R. Hakobyan[a], Roman B. Alaverdyan[a] & Rafik S. Hakobyan[ab]
[a] Yerevan State University, Yerevan, Republic of Armenia
[b] Beam Engineering for Advanced Measurements Co., Winter Park, Florida, USA
Published online: 30 Sep 2014.

Mol. Cryst. Liq. Cryst., Vol. 596: pp. 152–162, 2014

ISSN: 1542-1406 print/1563-5287 online
DOI: 10.1080/15421406.2014.918756

Thermomechanical Effects in Hybrid and Cylindrical-Hybrid Oriented Nematic Liquid Crystals

MARIAM R. HAKOBYAN,[1] ROMAN B. ALAVERDYAN,[1] AND RAFIK S. HAKOBYAN[1,2,*]

[1]Yerevan State University, Yerevan, Republic of Armenia
[2]Beam Engineering for Advanced Measurements Co., Winter Park, Florida, USA

It is observed and theoretically and experimentally studied thermomechanical flow in hybrid and cylindrical-hybrid oriented nematic liquid crystals (NLCs). The latter corresponds to the cell with homeotropic and axial boundary conditions on the substrates. The thermomechanical flow and rotation of NLC in such cells proceeds due to vertical temperature gradient. We suggest an experimental set up, a new configuration of NLC, for testing one of the twelve relations between twelve thermomechanical coefficients. In order to check the remaining relations between those coefficients it is important to have various configurations of NLC possible via photoalignment technology.

Keywords Hydrodynamics; thermomechanics; nematic liquid crystals

I. Introduction

Development of biomimetic, stimuli responsive, smart materials has attracted significant interest from the materials research community [1, 2]. There have been considerable efforts to mimic the fiber structure of skeletal muscle by developing soft linear electromechanical and/or thermomechanical actuators as the building blocks of artificial muscles [3, 4]. Some possibilities for modeling of artificial muscles are to find convenient transduction mechanisms of electric, thermal or light energy into mechanical work. In many cases even photomechanical transformation is carried out through intermediate thermal conversion. Although since 2001 appeared works of some groups where they reported on trans to cis isomerization mechanism of photomechanical transformation (see e.g. [5–11]). In various systems of low-molecular-weight liquid crystals (LC), LC polymers, LC elastomers and LC block copolymers, photocontrollable LC actuators have been achieved by introduction of photochromic molecules into LC materials. Light can conveniently manipulate order–disorder and order–order changes of LC materials, which induces photochemical phase transition and photoinduced cooperative motion, leading to their photonic applications. Through crosslinking LC elastomers give birth to photomechanical and photomobile effect in macroscopic scales. Unfortunately, to the best of our knowledge, still don't exist

*Address correspondence to Rafik S. Hakobyan, Beam Engineering for Advanced Measurements Co., 809 South Orlando Ave., Suite I, Winter Park, Florida 32789, Tel.: (407) 629-1282; Fax: (407) 629-0460. E-mail: rhakob@beamco.com

fundamental theory for trans to cis isomerization mechanism of photo/thermomechanical effects.

On the contrary, thermomechanical effects were predicted for deformed nematic liquid crystals (NLCs) in [12], where the first consistent theory of thermomechanical coupling due to nonuniform director orientation under a temperature gradient was developed for uniaxial nematics. The same terms in the thermomechanical equations were written and predicted new electromechanical effects in [13]. These thermomechanical coupling (including photoinduced) was observed in numerous experimental studies [14–17], and the measured values of thermomechanical coefficients were in good agreement with the theoretical estimates obtained in [12].

In [18, 19] they studied thermomechanical hydrodynamical flow and reorientation of director of compressible hybrid-oriented NLC cell under the influence of a temperature gradient directed normal to the restricting surfaces, when the sample is heated both from below and above. Calculations show that under the influence of temperature gradient the compressible NLC sample settles down to a stationary flow regime, both with the horizontal u and vertical w components of velocity $\mathbf{v}$, and u is directed in the opposite direction, approximately one order of magnitude less, than the one in the case of an incompressible NLC cell. The case of the orientational thermoelastic interaction considered in [20], which has not been discussed in the literature earlier, belongs to the effects in open systems and is quadratic in the temperature gradient. This type of interaction was registered experimentally and described in [21]. In [22] have been successfully dispersed gold nanoparticles AuNP in thermomechanical NLC elastomer actuators and had significantly improved the material response to a thermal stimulus. Embedment of AuNPs in NLC stiffened the elastomers, resulting in a slight decrease in the strain of the actuators, but this effect was more than compensated by a significant improvement in the actuator strain rate in response to an external stimulus. Incorporating a fractional amount of metal nanoparticles in these thermomechanical actuators can result in a pronounced enhancement of the thermal conductivity.

As we have shown, in the case when the thermomechanical hydrodynamic flow tends to reduce the curvature of the "flexible ribbon" of hybrid or cylindrical-hybrid oriented NLC, an oscillatory motion was predicted and observed [15, 23]. In the hybrid aligned cell an oscillatory motion was observed. And in the cylindrical-hybrid aligned cell a clockwise and counterclockwise oscillatory rotations were observed and studied.

In this paper new results on the thermomechanical effect in hybrid and cylindrical-hybrid oriented horizontal layers of NLC due to a vertical temperature gradient has been presented. We studied theoretically and experimentally the possibility of hybrid curvature reversal due to the hydrodynamic flow. This model allows us to explain our previous experimental results about oscillatory hydrodynamic flow due to the thermomechanical forces at the presence of a transverse temperature gradient, to do new predictions for experimental situation where present thermome-chani-cal coefficients differs from measured before.

II. Thermomechanical Equations in Hybrid and Cylindrical-Hybrid NLC

Let us consider an NLC cell having the so-called hybrid or cylindrical-hybrid orientation (Figs. 1, 2). We direct the normal to the cell walls and the cylindrical axis along the z axis, vertically upwards and assume that the boundary condition on the wall specifies homeotropic orientation $\mathbf{n}\,(z = 0) = \mathbf{e_z}$ at $z = 0$, where $\mathbf{n}$ is the director unit vector, with $\mathbf{n}$

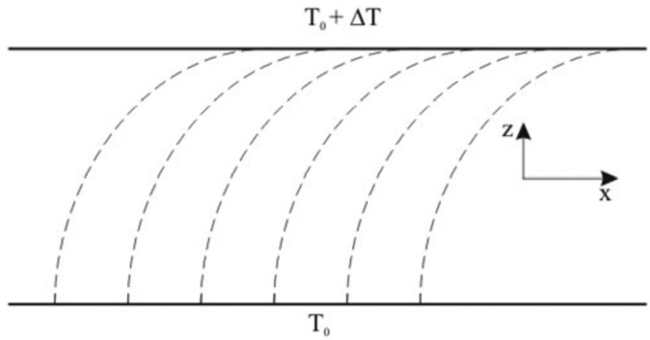

Figure 1. Director profile in a nematic LC cell with hybrid orientation and homogeneous temperature.

and –**n** equivalent, L is the cell thickness. For the cell with hybrid orientation we have planar orientation **n** (z = L) = $\mathbf{e_x}$ at z = L, and for the cell with cylindrical-hybrid orientation we have axial orientation (director **n** is directed along the tangents of coaxial circles).

In the case of cylindrical-hybrid initial orientation the problem's symmetry evidence that everywhere the vector **n** lays on the surfaces of coaxial cylinders with a general axis along *z*. It is evident also, that on the axis of cylinders the direction of **n** will be undefined, therefore that axis is a disclination. That is why the solution of the problem about the director distribution is applicable and valid only in the interval $a < r < R$, where a is of the micron size, R is the cylinder radius.

Let us introduce angle θ between director and z axis. Then in the case of hybrid initial orientation $n_x = \sin\theta(z)$, $n_y = 0$, $n_z = \cos\theta(z)$ and in the case of cylindrical hybrid orientation let's introduce a cylindrical coordinate system: r, φ, z. The problem's symmetry evidence, that in the second case the director unperturbed distribution does not depend on r and φ. Then the components of vector **n** one may write out in the following form: $n_\varphi = \sin\theta(z)$, $n_r = 0$, $n_z = \cos\theta(z)$. The boundary conditions for function $\theta(z)$ will be written in the simple form: $\theta(0) = 0$, $\theta(L) = \pi/2$, where L is the thickness of NLC layer.

Let the external heat sources maintain temperature $T = T_0$ at the plane $z = 0$ and temperature $T = T_0 + \Delta T$ at the plane $z = L$. The temperature gradient $dT/dz \sim \Delta T/L$ leads then, according to [12], to tangential thermomechanical stresses $\sigma^{thm}_{zx(\varphi)} \approx \xi\Delta T/L^2$, where ξ is the thermomechanical constant. The result is liquid flow in the x direction or rotation around cylindrical axis (in the second case). The stationary linear velocity **v** in this flow can be roughly estimated by equating the thermomechanical and Navier-Stokes contributions in the stress tensor σ_{ik}. Assuming for the latter $\sigma'_{zx(\varphi)} \approx \eta$v/L, where η is

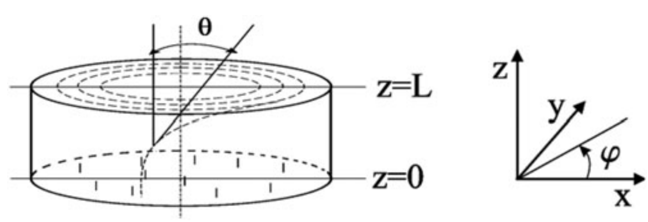

Figure 2. The cell of cylindrical-hybrid oriented NLC.

viscosity, we obtain $v \approx \xi\,\Delta T/L\eta$. This hydrodynamic flow leads to the reorientation of the NLC director. The direction of the flow velocity depends on the director concavity and the temperature gradient direction. If the temperature gradient is directed from the cell wall with planar (or axial) boundary condition to the wall with homeotropic condition, then thermomechanical hydrodynamical flow tends to increase the curvature of the "flexible ribbon" of hybrid NLC. If the temperature gradient has opposite direction then flow tends to reverse the curvature of "flexible ribbon". In the latter case thermomechanical stress induced the oscillatory hydrodynamical flow.

In order to describe the above mentioned thermomechanical effects we need to write equations of nematodynamics taking into account the thermomechanical stress tensor. They are balance equation of torque acting on NLC director and the Navier-Stokes equation.

Torque balance equations can be obtained from the variation principle [24]:

$$\prod_{ij}\left[\frac{\delta F}{\delta n_j} - \frac{\partial}{\partial x_k}\frac{\delta F}{\delta\left(\partial n_j/\partial x_k\right)} + f_j\right] = 0, \tag{1}$$

where $\prod_{ij} = \delta_{ij} - n_i n_j$ is the projection operator, $\mathbf{f}$ is the hydrodynamical "force" acting on the NLC director and expressed through the generalized velocities $\mathbf{N}$ and the velocity-gradient tensor d_{ij}:

$$f_i = (\alpha_3 - \alpha_2)\,N_i + (\alpha_3 + \alpha_2)\,d_{ij}n_j \tag{2}$$

$$N_i = \frac{dn_i}{dt} + \frac{1}{2}(\mathbf{n} \times \mathrm{curl}\mathbf{v})_i \qquad d_{ij} = \frac{1}{2}\left(\frac{\partial \mathrm{v}_i}{\partial x_j} + \frac{\partial \mathrm{v}_j}{\partial x_i}\right) \tag{3}$$

Here F is the free-energy density in its usual Frank's form:

$$F = \frac{1}{2}K_1\,(\mathrm{div}\mathbf{n})^2 + \frac{1}{2}K_2\,(\mathbf{n}\cdot \mathrm{curl}\mathbf{n})^2 + \frac{1}{2}K_3\,(\mathbf{n}\times \mathrm{curl}\mathbf{n})^2 \tag{4}$$

where K_i are Frank's elastic constants, and α_i are Leslie coefficients of the NLC. The Navier-Stokes equation for hydrodynamic flow velocity $\mathbf{v}(\mathbf{r},t)$ of an incompressible NLC, with the presence of thermomechanical terms, are of the form

$$\rho\left(\frac{\partial \mathrm{v}_i}{\partial t} + (\vec{\mathrm{v}}\vec{\nabla})\mathrm{v}_\mathrm{i}\right) = \frac{\partial \sigma_{ki}}{\partial x_k}, \tag{5}$$

$$\sigma_{ki} = -p\delta_{ki} + \sigma_{ki}^{'} + \sigma_{ki}^{\mathrm{thm}},\ \mathrm{div}\,\mathbf{v} = 0, \tag{6}$$

where ρ is the density, $p(\boldsymbol{r}, t)$ is the hydrodynamic pressure determined from the same set of Eq. (5, 6) and the boundary conditions, σ_{ki}' is the viscous stress tensor, and $\sigma_{ki}^{\mathrm{thm}}$ is the thermomechanical stress tensor [12].

We consider the problem homogeneous in the (x, y) plane ($\partial/\partial x = \partial/\partial y = 0$) and the director distribution in the (x, z) plane ($n_y = 0$) in the case of hybrid initial orientation. We have the boundary conditions for θ mentioned above. Thermomechanical stress leads to the hydrodynamic flow or rotation with velocity $\mathbf{v}$ directed in x direction ($\mathbf{v} = \mathbf{e}_\mathrm{x}\mathrm{v}$). For this problem equation (1) for director $\theta(z)$ has the form

$$(\alpha_3-\alpha_2)\frac{\partial\theta}{\partial t}=\left(K_3\cos^2\theta+K_1\sin^2\theta\right)\frac{\partial^2\theta}{\partial z^2}-(K_3-K_1)\sin\theta\cos\theta\left(\frac{\partial\theta}{\partial z}\right)^2$$
$$+\left(\alpha_3\sin^2\theta-\alpha_2\cos^2\theta\right)\frac{\partial \mathrm{v}}{\partial z} \tag{7}$$

Equation (7) describes reorientation of the NLC director under the influence of the hydrodynamic velocity gradient. And for the velocity in the thermomechanical single-constant approximation ($\xi_1=\xi_2=\ldots=\xi_{12}=\xi$) we have

$$\rho\frac{\partial \mathrm{v}}{\partial t}=\eta\frac{\partial^2\mathrm{v}}{\partial z^2}-\frac{1}{4}\xi\frac{dT}{dz}\left[\left(5+2\sin^2\theta\right)\sin(2\theta)\left(\frac{\partial\theta}{\partial z}\right)^2+\left(5+\sin^2\theta\right)\sin^2\theta\frac{\partial^2\theta}{\partial z^2}\right], \tag{8}$$

where $\eta=\eta_2+(\eta_1-\eta_2)\sin^2\theta+\eta_4\sin^2(2\theta)$, $\eta_4=0.25\alpha_1$ and $\eta_1=0.5(\alpha_3+\alpha_4+\alpha_6)$, $\eta_2=0.5(\alpha_4+\alpha_5-\alpha_2)$, $\eta_3=0.5\alpha_4$ are the Miesowicz viscosity coefficients. Equations (7, 8) are generalized equations for the description of thermomechanical flow in a NLC with the director confined to the surface of hybrid orientation.

In the case of cylindrical-hybrid cell we have write the free energy in the cylindrical system of coordinate. By means of Euler-Lagrange variational equation [12] we obtain the first integral of motion: $\theta'(\delta F/\delta\theta')-F=const$, where $\theta'=d\theta/dz$. Then we can find $\theta(z)$ in the implicit form

$$z=\int_0^\theta\left\{\frac{\frac{R^2-a^2}{2}\left[K_1\sin^2x+K_3\cos^2x\right]}{const+\ln\left(\frac{R}{a}\right)\left[\frac{1}{4}K_2\sin^2(2x)+K_3\sin^4x\right]}\right\}^{\frac{1}{2}}dx. \tag{9}$$

The boundary condition: $\theta(0)=0$ is taken already into consideration in the expression (9), and from the condition $\theta(L)=\pi/2$ we should find the *const*. Numerical computation of the expression (9) by means of "Mathematica-5" package shows that the dependence $\theta(z)$ in good approximation is linear. In particular, in a single-constant approximation that dependence to a sufficient precision takes the form $\theta(z)=\pi z/(2\mathrm{L})$. For hydrodynamic flow velocity **v**, from the problem's symmetry, it is obvious that $\partial/\partial\varphi=0$, $v_r=v_z=0$ and $v_\varphi=r\omega(r,z)$, where $\omega(r,z)=\partial\varphi/\partial t$ is the angular velocity of NLC rotation. Finally, for the rotation angular velocity we obtain the following equation:

$$\rho r\frac{\partial\omega}{\partial t}=\left[3\eta_3+\eta_5\sin^2\theta\right]\frac{\partial\omega}{\partial r}+\left[(\eta_1-\eta_2)\sin(2\theta)+2\eta_4\sin(4\theta)\right]\theta' r\frac{\partial\omega}{\partial z}$$
$$+\left[\eta_3+\eta_6\sin^2\theta\right]r\frac{\partial^2\omega}{\partial r^2}+\eta r\frac{\partial^2\omega}{\partial z^2}-\frac{1}{4}\xi\frac{dT}{dz}\left\{2\sin^2\theta\left(5+\sin^2\theta\right)\frac{d^2\theta}{dz^2}\right.$$
$$\left.+\left(5+2\sin^2\theta\right)\theta'^2\sin(2\theta)-(3\sin^2\theta-2)\frac{\sin(2\theta)}{r^2}\right\}. \tag{10}$$

Here $\eta_5=1.5\alpha_6+0.5\alpha_3$ and $\eta_6=0.5(\alpha_3+\alpha_6)$. In the limit case when $\mathrm{R}\to\infty$ we can find equation for the velocity ($\mathrm{v}=\omega\mathrm{R}$) of thermomechanical hydrodynamic flow in the planar hybrid cell (8). The equation (10) represents a linear, second order elliptical type equation, for which we should formulate, the Dirichlet problem with four boundary conditions: $\omega(r,z=0)=\omega(r,z=L)=\omega(r=a,z)=\omega(r=R,z)=0$. These conditions

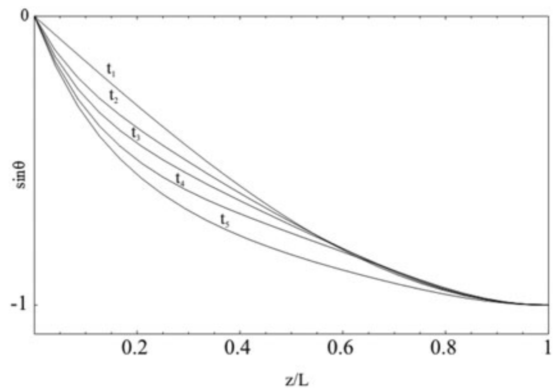

Figure 3. Profiles of the director's x component ($n_x = \sin\theta$) for different times (t_j) after switching the temperature gradient "on". The temperature gradient is directed from planar boundary to homeotropic one ($t_1 = 0$, $t_2 = 0.39$ sec, $t_3 = 0.77$ sec, $t_4 = 1.55$ sec, $t_5 = 7.74$ sec).

correspond to the NLC placed between two coaxial, hard cylinders with radiuses a and R and a height L. One may solve such kind of Dirichlet problem by means of the program "Mathematica-5". Numerical studies of the Eq. (10) have been carried out for the nematic liquid crystal MBBA. The results of computations are shown in Figs. 6, 7.

III. Thermomechanical Oscillation in Hybrid and Cylindrical-Hybrid NLC

Let us consider first the behavior of the hybrid NLC director in the presence of simple hydrodynamic flow, shear flow as an example ($v = v_0 z/L$, $v_0 = \text{const}$). The boundary conditions for the orientational angle are: $\theta(z = 0, t) = 0$ and $\theta(z = L, t) = \pm\,\pi/2$ ("+"if the "flexible ribbon" is oriented in the positive direction of x, and "–" otherwise). In the absence of flow the stationary solution of equation (7) with mentioned boundary conditions has, in good approximation, linear profile: $\theta(z) = \pm\,\pi z/(2L)$. Thus we can assume this solution as an initial condition for the general problem. Let us note that the equation (7) takes the form of the well-known "damped driven sine-Gordon equation" in the single-constant approximation for elastic constants ($K_1 = K_3$). We were able to solve equation (7) for director reorientation under the influence of flow with the above-mentioned boundary and initial conditions using "Mathematica-5". In this calculation for NLC MBBA (because only for it we have all hydrodynamical constants) we assumed $K_1 = 6{\cdot}10^{-7}$erg/cm; $K_3 = 7.5{\cdot}10^{-7}$erg/cm; $\alpha_2 = -\,0.77$P; $\alpha_3 = -\,0.012$P. If hydrodynamic flow velocity is directed out of the "flexible ribbon's" curvature (in the opposite direction of x axis on the Fig. 1), then velocity gradient brings about a small increase of curvature (see Fig. 3). The curvature deforms more completely and the deformation increases in time when velocity is directed into (in the direction of x axis) "flexible ribbon's" curvature (Fig. 4). Thereby director deformation elastic energy F increases in time, where

$$F = \frac{1}{2}\left(K_1 \sin^2\theta + K_3 \cos^2\theta\right)\left(\frac{\partial\theta}{\partial z}\right)^2 \tag{11}$$

The "flexible ribbon" reverses its curvature at the time when deformation energy becomes larger than surface anchoring energy at z = L. In that way velocity is directed out of the

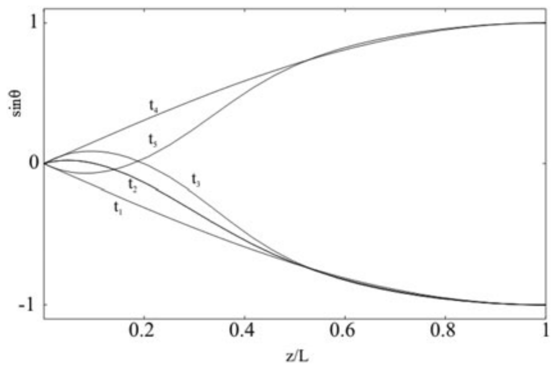

Figure 4. Profiles of the director's x component ($n_x = \sin\theta$) for different times (t_j) after switching the temperature gradient "on". The temperature gradient is directed from homeotropic boundary to planar one ($t_1 = 0$, $t_2 = 0.77$ sec, $t_3 = 1.55$ sec, $t_4 = 3.35$ sec, $t_5 = 4.64$ sec). Reversal time is $t_r = 3.35$ sec and oscillation period is $\tau_p = 6.7$ sec.

reversed curvature. The reversing time depends on NLC parameters and surface coupling energy. Later depends on the method of surface treatment.

Now let us consider the thermomechanical effect in a hybrid-oriented nematic with initial director distribution $\theta(z, t = 0) = \pm\,\pi z/(2L)$. Let the condition $T\ (z = 0) > T\ (z = L)$ be satisfied for the temperatures kept on the NLC cell substrates. Then, in the presence of the gradient of the director orientation angle along the z-coordinate, a thermomechanical hydrodynamic flow appears, which moves along the x axis at the velocity v. When we have initial condition $\theta(z,\ t = 0) = \pi z/(2L)$ the "flexible ribbon" convexity is directed opposite to the positive x direction (as in Fig. 1). The thermomechanical hydrodynamical flow is directed in the same way, out of the "flexible ribbon's" curvature and causes a little deepening of the curvature. When we have initial condition $\theta(z,\ t = 0) = -\,\pi z/(2L)$, the "flexible ribbon" convexity is directed along the positive x direction. The thermomechanical hydrodynamical flow is directed in the same way and again causes some deepening of curvature. Let us heat the same cell from the wall with z = L: $T\ (z = 0) < T\ (z = L)$. Then for both initial conditions the thermomechanical hydrodynamical flow is directed into "flexible ribbon's" curvature and deforms it completely. This deformation increases in time and induced the reversal of curvature. This leads to velocity reversal. That is why in this reverse case of curvature and velocity thermomechanical velocity again has the direction into the "flexible ribbon's" curvature and so it again causes a reversal of curvature and velocity. Thereby we can observe oscillatory thermomechanical motion, the period of which is equal to twice the time of the first reversal of curvature or velocity. This oscillatory behavior of NLC director orientation and thermomechanical hydrodynamical velocity can be described by the system of equations (7) and (8). The boundary conditions for velocity are v(z = 0, t) = v(z = L, t) = 0 and initial condition v(z, t = 0) = 0. For calculation with "Mathematica-5" we assume for NLC MBBA $\rho = 1\text{g/cm}^3$, $\xi = 10^{-6}\text{erg/cm}\cdot\text{K}$, $\Delta\text{T} = 10\text{K}$. As we have mentioned above, surface anchoring energy depends on the method of surface treatment. It can be several times larger than the deformation free energy F for a stationary distribution of the NLC director. In our calculation we will take it as twice larger than the deformation energy for initial stationary distribution. As we have mentioned above, the period of oscillation is twice of the reversal time. So for the cell thickness $\text{L} = 10^{-2}$ cm we obtain a period of $\tau_\text{p} = 6.7$ sec. The oscillation period strongly

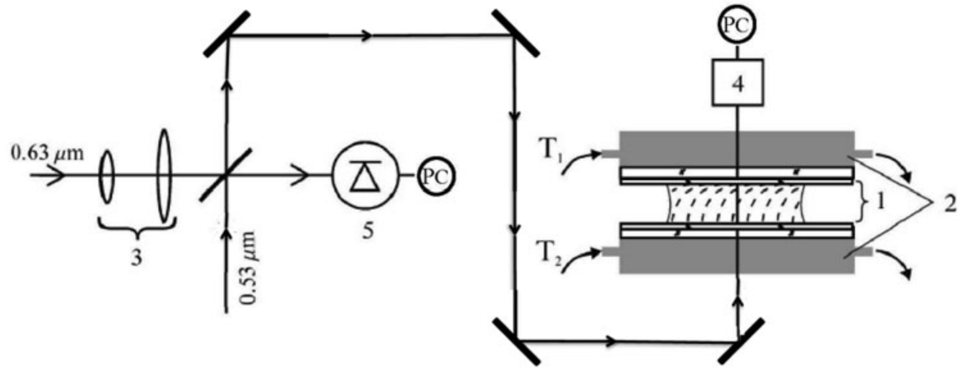

Figure 5. The arrangement of the experimental setup. 1—the hybrid or cylindrical-hybrid oriented NLC cell, 2—circulating water with two regulative thermostats, by the help of which the temperature gradient ($T_1 - T_2$) is set in, 3—telescopic widener of the probe laser beam, 4—a CCD camera for the observation of hydrodynamic fluxes, and 5—photodetector for the Nd YAG laser intensity control.

depends on the surface coupling energy. The hybrid NLC director distribution cannot exist when the surface coupling energy is less than the free energy of initial stationary director's distribution (in our case it was 1.25×10^{-2}erg per cm^2 of cell surface). This oscillation period strongly increases with an increase of the surface coupling energy from its minimal value.

In the case of cylindrical-hybrid initial NLC orientation we have similar situations for rotational motions. When we heat from the bottom side we get deepening of hybrid curvature. And by heating from above we get oscillatory thermomechanical rotation in clockwise and counter clockwise directions.

IV. Experiments on Thermomechanical Effects in Hybrid and Cylindrical-Hybrid Oriented NLC

Hybrid and cylindrical-hybrid oriented NLC MBBA cells with a phase transition temperature interval 20–47°C were used in the experiment. The arrangement of the experimental setup is sketched in Fig. 5. The "sandwich"-type cells were arranged such that they were strictly horizontal. The vertical temperature gradient was created with the help of circulating water with two regulative temperatures. The heat conductivity of cell plates exceeds the heat conductivity of nematic by $2 \div 3$ times. This significant condition was provided in order to ensure constant boundary conditions for temperature. The visualization of hydrodynamic flow was provided by adding some aluminum powder with a concentration about 10^{-3} wt% in the nematic. The hydrodynamic fluxes were observed with the help of a probe He–Ne laser beam. The motion of aluminum oxide particles was registered by a CCD camera (4) which was interfaced to a PC. The temperature difference varied from 0°C to 10°C with errors of about 0.1°C. The maximum velocity along the z coordinate, was defined as the maximum velocity of the small ($2 \div 3$ μm) aluminum oxide particles. The thickness of the cells was $L = 100$ μm and the radius of external cylinder was $R = 1.6$ cm.

In the experiment with a hybrid cell, when the planar oriented plate was located on top and the cell was heated from below, NLC flow along the x direction was observed. This flow was directed perpendicular to the temperature gradient in the plane of the director distribution and was conserved at the cell, slewing around the z axis. The maximum velocity

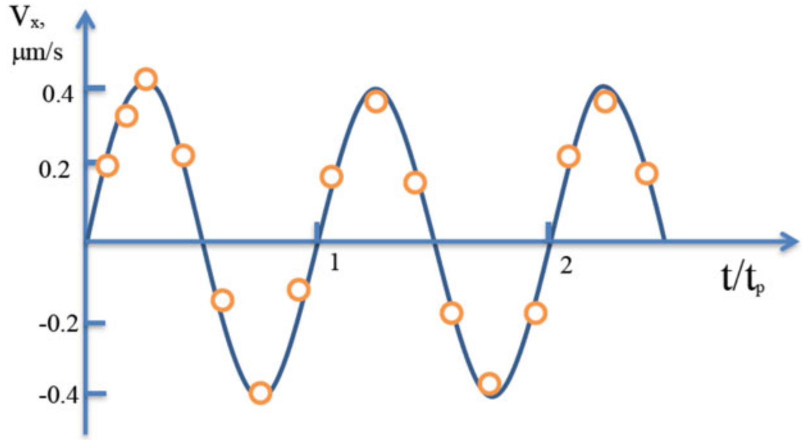

Figure 6. Dependence of x component of velocity on time.

of the hydrodynamic flow was of order $v = 0.4$ μm/s, with a temperature difference $\Delta T = 5°$C. This flow was interrupted when the NLC reached the end of the cell, due to capillary forces. NLC was not returned to the initial position when the temperature gradient was switched off. Through experimental results we can estimate the thermomechanical constant $\xi \sim 10^{-7}$ dyne/K. In the experiment with a hybrid-oriented cell, when the homeotropically oriented plate was located on top and the cell was heated from below, oscillatory NLC flow was observed. Starting its motion along the x direction, the NLC reversed direction after 15 – 20 min. This process recurs infinitely (see Fig. 6).

In the experiment with a cylindrical-hybrid NLC cell, arranged as in the first case, rotation of NLC around the cylinder axis was observed. The linear velocity of the rotation was constant along the z axis in the volume of NLC and vanished at the $z = 0$, L. The dependence of the maximum velocity along the z coordinate on the distance r from the

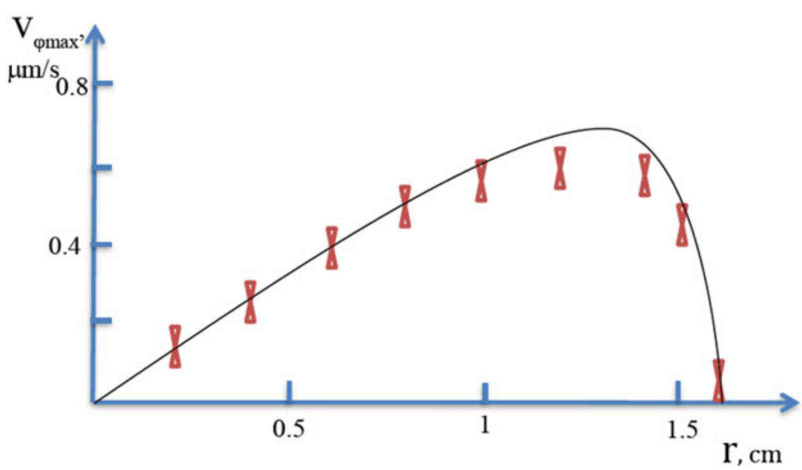

Figure 7. The maximal with respect to z linear velocity dependence on the distance r from the axis of cylinders, when $\Delta T = 5°$C.

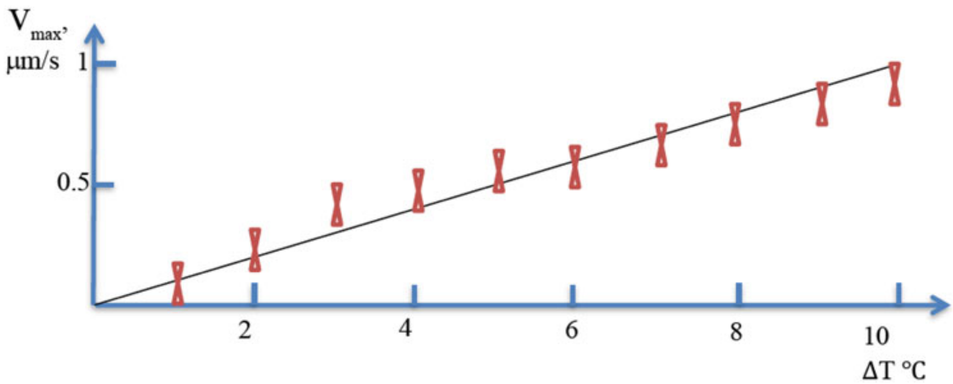

Figure 8. The maximal with respect to z and r linear velocity dependence on the temperature difference ΔT.

cylinder axis, with a temperature difference of $\Delta T = 5°\text{C}$, is shown in Fig. 7. It is seen that there is good agreement of theoretical assumptions and experimental results if we take the thermomechanical coefficient $\xi = 0.22{\cdot}10^{-6}$ dyne/K. The dependence of the maximum (along z and r) velocity on the temperature difference ΔT is linear, in accordance with the theoretical assumptions (see Fig. 8). When the planar oriented plate was located on the bottom and the cell was heated from below, an oscillatory rotation of NLC around the axis of the cylinder was observed.

When we increased the temperature gradient, transition to orientational turbulence was observed and, finally, we had a chaotic distribution of NLC director. In turn, the orientational turbulence leads quickly to a hydrodynamic turbulence. In the case of such temperature gradients, the investigation of the system becomes very difficult because its behavior is unpredictable.

IV. Conclusion

We have observed and studied thermomechanical flows, rotations and oscillations in hybrid and cylindrical-hybrid oriented NLC. The good agreement between the theoretical assumptions and experimental results prove ones more the validity of the predictions in [12]. It was revealed that the steady state hydrodynamic flow with the magnitude and direction dependent on the temperature gradient ΔT and the character of the anchoring of the liquid crystal molecules to the bounding surfaces of cell is induced under the effect of the temperature gradient ΔT directed perpendicular to these surfaces. Numerical calculations and observations demonstrated that the change in the character of the anchoring of the liquid crystal molecules from homeotropic to planar at the warmer bounding surface of the cell and from planar to homeotropic at the colder surface leads to qualitative and quantitative changes in the relaxation of the field velocity, which results in the formation of oppositely directed steady state hydrodynamic flows. All these facts allowed us to establish a number of specific features that are associated with the response of liquid crystal materials to the action of the temperature gradient and should be taken into account in the design of sensors or liquid crystal displays.

In the future, if we disperse nanoparticles in NLC, we can have significantly improved the material response to a thermal stimulus. Embedment of nanoparticles in NLC will stiffen the molecules, resulting in a significant improvement in the thermal–order–mechanical coupling behavior and external field-induced thermomechanical effects. Incorporating a fractional amount of metal nanoparticles in NLC can result in a pronounced enhancement of the thermal conductivity.

An investigation of these effects may, in our opinion, yield new important information on the molecular dynamics of the mesophase of liquid crystals.

Acknowledgments

This work was supported by State Committee Science MES RA, in frame of the research project No. SCS 13-1C061. The authors are grateful to B. Ya. Zeldovich and N. V. Tabiryan for very useful discussions.

References

[1] Hashimoto, S., Yusuf, Y., Krause, S., Finkelmann, H., Cladis, P., Brand, H., & Kai, S. (2008). *Applied Physics Letters*, *92*, 181902.
[2] Spillmann, C., Konnert, J., Deschamps, J., Naciri, J., & Ratna, B. (2008). *Chemistry of Materials*, *20*, 6130.
[3] Kottke, E., Partridge, L., & Shahinpoor, M. (2007). *Journal of Intelligent Material Systems and Structures*, *18*, 103.
[4] Shenoy, D., Thomsen, III D. L., Srinivasan, A., Keller, P., & Ratna, B. (2002). *Sensors & Actuators A: Physica*, *l* 96, 184.
[5] Finkelmann, H., Nishikawa, E., Pereira, G. G., & Warner, M. (2001). *Phys. Rev. Lett.*, *87*(1), 015501/1.
[6] van Oosten, C. L., Corbett, D., Davies, D., Warner, M., Bastiaansen, C. W. M., & Broer, D. J. (2008). *Macromolecules*, *41*(22), 8592.
[7] White, T. J., Tabiryan, N., Tondiglia, V. P., Serak, S., Hrozhyk, U., Vaia, R. A., & Bunning, T. J. (2008). *Soft Matter*, *4*, 1796.
[8] White, T. J., Serak, S. V., Tabiryan, N. V., Vaia, R. A., & Bunning T. J. (2009). *J. Mater. Chem.*, *19*(8), 1080.
[9] Lee, K. M., Koerner, H., Vaia, R. A., Bunning, T. J., & White, T. J. (2010). *Macromolecules*, *43*, 8185.
[10] Yu, Y., & Ikeda, T. (2011). *Adv. Mater.*, *XX*, 1.
[11] Lee, K.M., Tabiryan, N.V., Bunning, T. J., and White, T. J. (2012). *J. Mater. Chem.*, *22*(2), 691.
[12] Akopyan, R. S., & Zel'dovich, B. Y. (1984). *Sov. Phys. JETP*, *60*, 953.
[13] Brand, H. R., & Pleiner, H. (1987). *Phys. Rev. A*, *35*, 3122.
[14] Lavrentovich, O. D., & Nastishin, Yu. A. (1987). *Ukr. Fiz. Zh.*, *32*, 710.
[15] Akopyan, R. S., Alaverdyan, R. B., Chilingaryan, Yu. S., & Santrosyan, E. A. (2001). *J. Appl. Phys.*, *90*, 3371.
[16] Poursamad, J. B., Aleksanyan, A. K., & Hakobyan, R. S. (2010). *J. Appl. Phys.*, *108*, 123113–1.
[17] Hakobyan, R. S., Alaverdyan, R. B., Gevorgyan, G. S., & Kirakosyan, A. A. (2010). *JETP Letter*, *92*(7), 504.
[18] Zakharov, A.V., & Vakulenko, A. A. (2009). *Phys. Rev. E*, *79*, 011708.
[19] Zakharov, A. V., & Vakulenko, A. A. (2009). *Phys. Rev. E*, *80*, 031711.
[20] Trashkeev, S. I., & Britvin, A. V. (2011). *Tech. Phys. 56*(6), 747.
[21] Demenev, E. I., Pozdnyakov, G. A., & Trashkeev, S. I. (2009). *Tech. Phys. Lett.*, *35*, 674.
[22] Montazami R., Spillmann C. M., Naciri J., & Ratna B. R. (2012). *Sensors and Actuators A: Physical*, *178*, 175.
[23] Hakopyan, R. S., Yesayan, G. L., & Zel'dovich, B.Y. (2006). *Phys. Rev. E*, *73*, 061707.
[24] Akopyan, R. S., & Zel'dovich, B. Y. (1984). *Sov. Phys. JETP*, *59*, 311.